Development of Time- and Energy-Resolved Synchrotron-Radiation-Based Mössbauer Spectroscopy

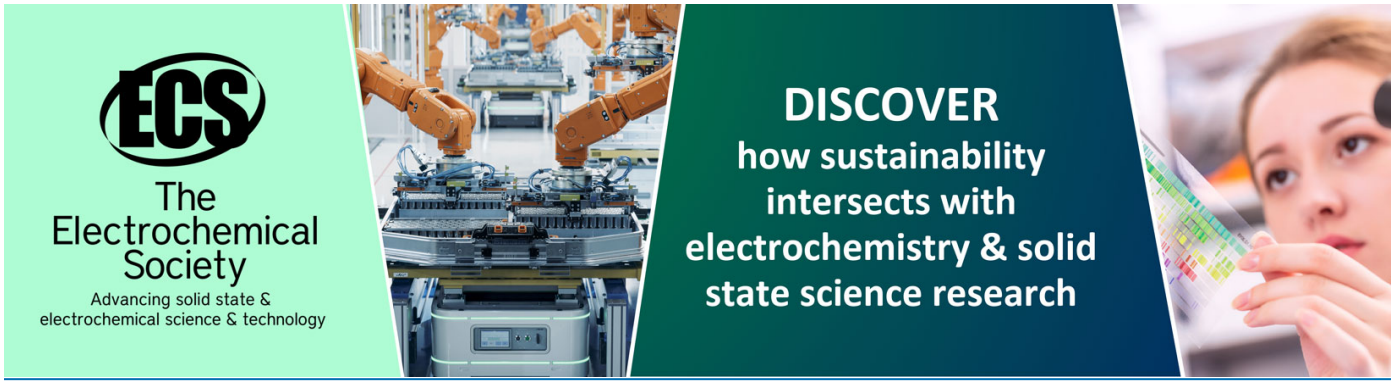

Journal of Physics: Conference Series **2380** (2022) 012136 doi:10.1088/1742-6596/2380/1/012136

Development of Time- and Energy-Resolved Synchrotron-Radiation-Based Mössbauer Spectroscopy

S. Kitao[1*)], R. Masuda[2], T. Fujihara[3], H. Tajima[3], N. Nagasawa[4], Y. Yoda[4], T. Masuda[5], K. Yoshimura[5], and M. Seto[1]

[1]Institute for Integrated Radiation and Nuclear Science, Kyoto University, Kumatori, Osaka 590-0494, Japan
[2]Faculty of Science and Technology, Hirosaki University, Hirosaki, Aomori, 036-8561, Japan
[3]Graduate School of Science, Kyoto University, Kyoto 606-8502, Japan
[4]Japan Synchrotron Radiation Research Institute, Sayo, Hyogo 679-5198, Japan
[5]Research Institute for Interdisciplinary Science, Okayama University, Okayama 700-8530, Japan

[*)]E-mail: kitao.shinji.5s@kyoto-u.ac.jp

Abstract. Synchrotron-radiation based Mössbauer spectroscopy has become a useful technique capable for investigating various Mössbauer isotopes. For a typical experimental setup, the information associated with the pulse height (that is, energy) in an avalanche photodiode (APD) detector has not been used effectively. By using a system for simultaneous measurement system of time and energy associated with the APD signal, a system for the time- and energy-resolved Mössbauer spectroscopy has been developed. In this system, the pulse height information was converted to the time information through an amplitude-to-time converter applied to one of the divided signals from the APD. The corresponding time information was processed separately from another one of the divided signals. Both signals are recorded by a multi-channel scaler in an event-by-event data acquisition process. The velocity information from the Mössbauer transducer was also recorded as a tag for each signal event. Thus, the Mössbauer spectra with any time- and energy-window can be reconstructed after the data collection process. This system can be used for many purposes in time- and energy-resolved Mössbauer spectroscopy, and shows significant promise for use with other fast detectors and for various types of experiments.

1. Introduction

Mössbauer spectroscopy is one of the most powerful methods of extracting the information associated with the electronic states or magnetic states of a specific isotope. For conventional methods of Mössbauer spectroscopy, radioactive nuclides are used to excite the Mössbauer isotopes. On the contrary, synchrotron radiation (SR) can be used to excite the Mössbauer levels instead of radioactive sources during nuclear resonant scattering (NRS) experiments. In the NRS experiments, the NRS signals must be distinguished from considerably stronger electronic scattering signals. This distinction is typically achieved through a timing method using an avalanche photodiode (APD) detector, which has a high time resolution on the order of several hundred picoseconds. The NRS signal is scattered with a delay corresponding to the half-life of the excited isotope, while the electronic scattering occurs

promptly. The NRS experiment can be performed in the time domain, since the time spectra from the nuclear resonant forward scattering process contains information about the Mössbauer parameters. Nevertheless, another useful method, i.e., SR-based Mössbauer spectroscopy, which is applicable to almost every Mössbauer isotope, has been developed [1]. A typical experimental setup of this method is shown in Fig. 1. A monochromatized SR beam leads to two samples, a transmitter and a scatterer. The scattered signals from the scatterer are collected by an APD detector. The NRS signal is distinguished from electronic signals with a certain time window. The transmitter or the scatterer is moved by a transducer, which is used for an energy-domain scan based on a Doppler velocity as in the case of conventional Mössbauer spectroscopy. The transmitter or the scatterer is taken as the reference sample with a single-line Mössbauer absorption spectrum. When the relative Doppler velocity of the transmitter and the scatterer matches the energy position of Mössbauer absorption, scattered counts of the NRS signal decrease. Thus, this method can obtain energy-domain absorption spectra similar to those obtained via conventional Mössbauer spectroscopy. The SR-based Mössbauer spectroscopy technique is employed in many experiments on various samples under various conditions. Recently, several Mössbauer isotopes (e.g., ^{174}Yb[2] and ^{161}Dy[3]) have been investigated using this technique.

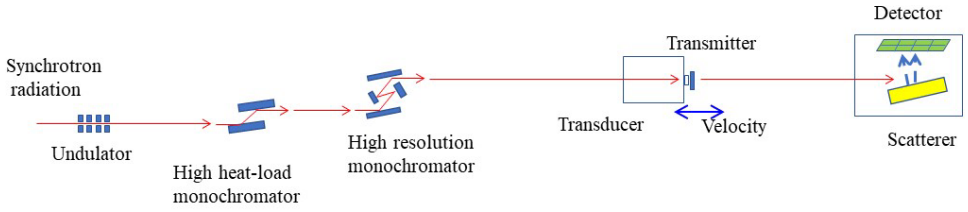

FIGURE 1. Typical experimental setup of SR-based Mössbauer spectroscopy.

The scattered NRS signal collected by the APD detector contains not only γ-rays with the excited energy but also fluorescent x-rays and conversion electrons emitted from the internal conversion process of the excited level. The detection efficiency of the APD detector is higher for lower energy x-ray and electrons, and therefore any of the scattered signals can be utilized. Although the scattered signals associated with different energies contain different information, effective use of this information is lacking so far. The pulse height of the APD signal contains information regarding the energy of the detected signal, thereby allowing the energy-resolved treatment of the APD signal. One difficulty encountered in using the pulse-height information in this experiment results partly from maintaining a high time resolution even after treatment of the signal. To realize the time- and energy-resolved signal treatments simultaneously, we introduced an amplitude-to-time converter (ATC) and developed an event-by-event data collection system [4]. This system has been successfully used to excite the second excited state of ^{229}Th by SR [5]. In this study, an experiment employing depth-selective Mössbauer spectroscopy was demonstrated by using the time- and energy-resolved system. The time and energy selectivity of the present system will allow the use of this novel Mössbauer spectroscopy for various applications in new fields.

2. Experimental

An electron-beam gun deposition system was used to prepare a sample to demonstrate the depth-selective experiment. Eu metal (thickness: ca. 300 nm), Cr metal (300 nm) and EuF_3 (100 nm) were successively deposited onto a Si substrate. The experiment was performed at BL35XU, an undulator beamline at SPring-8 (Super Photon ring, 8 GeV). The x-ray energy was tuned to 21.541 keV of ^{151}Eu nuclear resonant energy. The energy width of the x-ray was monochromatized to 1.7 meV with a high-heat-load monochromator with Si(1 1 1) crystals and a high-resolution monochromator with nested Si(4 2 2) and Si(12 12 8) crystals. In addition, the measurement system was developed and the proportionality of the ATC delay time and incident energy was confirmed at Photon Factory (PF) BL-

14A beamline at High Energy Accelerator Research Organization (KEK). The preparatory experiments were also performed at BL09XU and BL11XU at SPring-8.

A schematic diagram showing the time- and energy- resolved measurement system is presented in Fig. 2. The signal from an APD detector was amplified by a set of pre-amplifiers and a variable attenuator was inserted to adjust the pulse height in the appropriate energy range. The signal was divided into two signals by a divider. One signal (hereafter, ch 1), which is connected to the multi-channel scaler (MCS, FAST Comtec, MCS6) with a 0.1 ns time-bin width, is treated regularly to obtain time information. The other signal (ch 2) is connected to the ATC module, which is sufficiently fast to treat signal rates on the order of MHz. Operation of the ATC requires another input signal, which coincided with the ch 1 signal. In order to reduce unnecessary prompt signals, signals coinciding with the incident SR were inhibited (veto) using the timing signal of the SR ring operation. The output signal of the ATC was delayed with a certain time (this time delay is proportional to the pulse height). Thus, the energy information was converted to the timing information. Each timing signal was recorded by the MCS in the list-mode during an event-by-event data acquisition process. The velocity information was also recorded as a tag for each signal, through a tag converter module from the function generator of the velocity transducer. The energy information is extracted from the time difference of ch 1 and ch 2. Furthermore, during the analyses, the correspondence between ch 1 and ch 2 signals was chosen from the order of the signal. The obtained set of signals has three-dimensional information (time, energy, and velocity). After the data collection process, Mössbauer spectra can be reconstructed using an arbitrary time window and energy window.

The multi-element APD detector used has eight elements (area of each element: 3x5 mm^2). In this experiment, four APD elements aligned along the beam direction were used and four sets of time- and energy-resolved system were individually prepared. The experiment was performed without evacuation of the sample chamber housing the APD detector. During the experiment, the APD detects 21.5 keV γ-rays and fluorescent x-rays (ca. 5.8 keV) from the internal conversion process; no conversion electrons are detected. A Eu-Cr-EuF_3 deposited Si plate was used as the scatterer and a EuF_3 was used as the transmitter. The experiment was performed at room temperature.

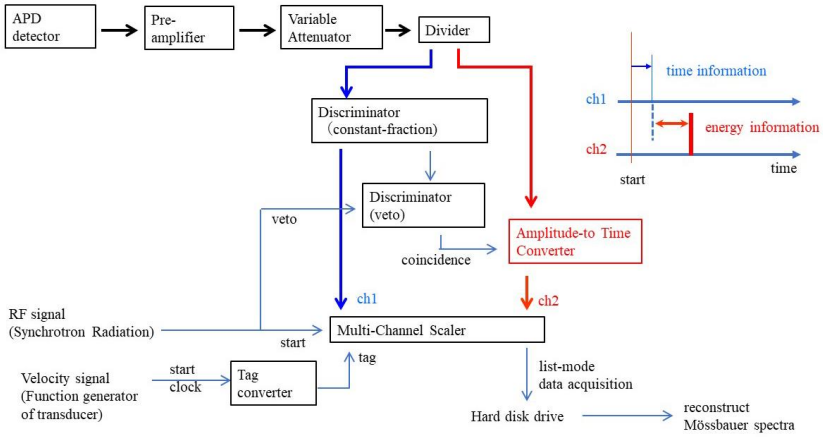

FIGURE 2. Schematic diagram for measurement system of time- and energy-resolved SR-based Mössbauer spectroscopy.

3. Results and Discussion

Figure 3 shows typical reconstructed energy spectra and Mössbauer spectra for different APD elements (i.e., element 1 and element 4). Each spectrum consists of two peaks corresponding to 5.8 keV and 21.5 keV. Two dips, which can be attributed to Eu^{2+} and Eu^{3+} components, occur in the obtained Mössbauer spectra. The Eu^{2+} component is associated with Eu metal occurring in the bulk of the sample, while the Eu^{3+} is generated mainly by a surface EuF_3. The Eu^{3+} component is partly

generated by oxidized Eu metal. Analysis of each energy spectrum has clarified that the shape of the Mössbauer spectra differs between the APD element. The changes in the energy distribution occurred by different acceptance angle of each element. The sample thickness for the element 4 was effectively thicker than the others because of lower acceptance angle. This energy analysis is quite difficult without the use of the present system.

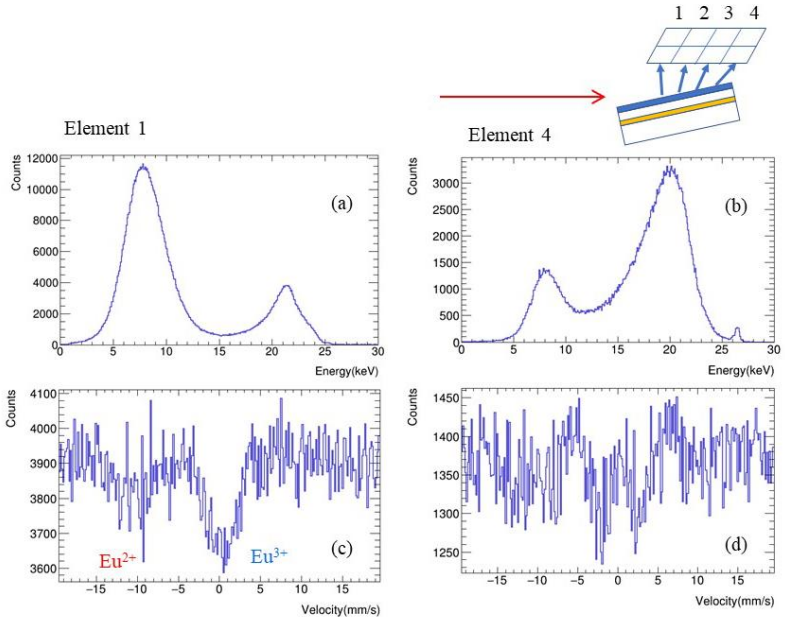

FIGURE 3. Typical reconstructed energy spectra (a and b) and Mössbauer spectra (c and d) for the APD elements 1 and 4, respectively.

The analysis confirmed that the difference between the Mössbauer spectra of the APD elements results from a mixture of the energy. Therefore, the signals of four APD elements were added to the subsequent analyses. Figure 4 shows typical energy-resolved reconstruction of Mössbauer spectra performed by choosing energy-windows that extract 5.8 keV and 21.5 keV separately using all data obtained for the four APD elements. The shape of the Mössbauer spectra differs among the elements. Regarding Eu^{2+} and Eu^{3+}, where dips occur in the 5.8 keV spectrum, the 5.8 keV x-rays originate mainly from the surface EuF_3, and hence the Eu^{3+} component is enhanced. However, the 21.5 keV spectrum reveals an enhancement of Eu^{2+}, which results mainly from non-surface Eu metal. The dip shape in the 21.5 keV spectrum has double hump character, while the 5.8 keV dip is characterized by a single line pattern. This feature results from the difference in the scattering processes (as discussed in previous work [6]). That is, the fluorescent x-rays were scattered incoherently, while the 21.5 keV γ-rays are associated with both an incoherent scattering process and a forward scattering process. Precise analyses of Mössbauer spectra with mixed energy can be performed using the energy-resolved Mössbauer spectroscopy employed in the present work.

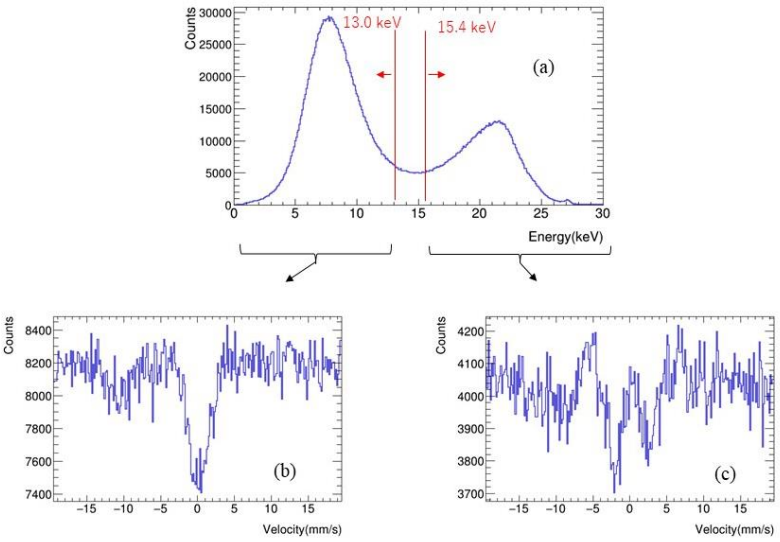

FIGURE 4. Energy spectrum of all APD elements(a). Energy-resolved Mössbauer spectra obtained at energies below 13.0 keV (b) and above 15.4 keV (c).

In summary, a measurement system of time- and energy-resolved SR-based Mössbauer spectroscopy is successfully developed. An example experiment for depth-selective Mössbauer spectroscopy is demonstrated. Through this method, time-resolved and/or energy-resolved Mössbauer spectroscopy can be applied to various application in new fields. Moreover, the developed system can be used for other fast detectors and various types of experiments.

Acknowledgements

The authors thank Prof. S. Kishimoto of KEK for helpful support for the experiments at PF of KEK. We also thank Dr. T. Mitsui and Dr. K. Fujiwara of National Institutes for Quantum and Radiological Science and Technology (QST) for helpful support with the preparatory experiment in BL11XU at SPring-8. The authors thank Dr. Y. Kobayashi and Dr. M. Kurokuzu at Institute for Integrated Radiation and Nuclear Science, Kyoto University, as well as Mr. H. Ishibashi, Mr. H. Taniguchi, and Mr. H. Yamashita at Graduated School of Science, Kyoto University for their experimental support and fruitful discussion. This work was supported by Japan Society for the Promotion of Science (JSPS) Grant-in-Aid for Scientific Research Grant nos. 19K05250, 19H00685, and 21H04473. This work was partly supported by SPIRITS 2021 of Kyoto University. This work has been performed by using facilities of the Institute for Integrated Radiation and Nuclear Science, and Research Center for Low Temperature and Materials Sciences, Kyoto University. The synchrotron radiation works were performed at BL09XU, BL11XU and BL35XU beamlines of SPring-8 with the approvals of the Japan Synchrotron Radiation Research Institute (Proposal Nos. 2019B1491, 2019B3581, 2020A1583, and 2021B1699) and PF BL14A beamline of KEK with the approval of the PF Program Advisory Committee (Proposal No. 2020G097). This work was also partly supported by QST through the QST Advanced Characterization Nanotechnology Platform under the remit of “Nanotechnology Plat-form” associated with the Ministry of Education, Culture, Sports, Science and Technology (MEXT), Japan (Proposal No. JPMXP09A19QS0022).

References

[1] M. Seto, R. Masuda, S. Higashitaniguchi, S. Kitao, Y. Kobayashi, C. Inaba, T. Mitsui, Y. Yoda, Phys. Rev. Lett. **102**, 217602 (2009).

[2] R. Masuda, Y. Kobayashi, S. Kitao, M. Kurokuzu, M. Saito, Y. Yoda, T. Mitsui, F. Iga, M. Seto, Appl. Phys. Lett. **104**, 082411 (2014).
[3] R. Masuda, S. Kitao, H. Tajima, H. Taniguchi, T. Mitsui, K. Fujiwara, Y. Yoda, N. Nagasawa, D. Ishikawa, A. Q. R. Baron, T. Yoshida, T. Sato, K. Katoh, H. Kobayashi, M. Seto, Hyperfine Interact. **243**, 17 (2022).
[4] T. Masuda, S. Okubo, H. Hara, T. Hiraki, S. Kitao, Y. Miyamoto, K. Okai, R. Ozaki, N. Sasao, M. Seto, S. Uetake, A. Yamaguchi, Y. Yoda, A. Yoshimi, K. Yoshimura, Rev. Sci. Instrum. **88**, 063105 (2017).
[5] T. Masuda, A. Yoshimi, A. Fujieda, H. Fujimoto, H. Haba, H. Hara, T. Hiraki, H. Kaino, Y. Kasamatsu, S. Kitao, K. Konashi, Y. Miyamoto, K. Okai, S. Okubo, N. Sasao, M. Seto, T. Schumm, Y. Shigekawa, K. Suzuki, S. Stellmer, K. Tamasaku, S. Uetake, M. Watanabe, T. Watanabe, Y. Yasuda, A. Yamaguchi, Y. Yoda, T. Yokokita, M. Yoshimura, K. Yoshimura Nature **573**, 238 (2019).
[6] M. Seto, R. Masuda, Y. Kobayashi, S. Kitao, M. Kurokuzu, M. Saito, S. Hosokawa, H. Ishibashi, T. Mitsui, Y. Yoda, K. Mibu, Hyperfine Interact. **238**,78 (2017).